Journal of Power Sources 180 (2008) 621–629

Contents lists available at ScienceDirect

Journal of Power Sources

journal homepage: www.elsevier.com/locate/jpowsour

A novel flow battery—A lead-acid battery based on an electrolyte with soluble lead(II) V. Studies of the lead negative electrode

Derek Pletcher[a,*], Hantao Zhou[a], Gareth Kear[b], C.T. John Low[b], Frank C. Walsh[b], Richard G.A. Wills[b]

[a] Electrochemistry and Surface Science Group, School of Chemistry, University of Southampton, Southampton SO17 1BJ, United Kingdom
[b] Energy Technology Research Group, School of Engineering Sciences, University of Southampton, Southampton SO17 1BJ, United Kingdom

ARTICLE INFO

Article history:
Received 4 January 2008
Received in revised form 5 February 2008
Accepted 15 February 2008
Available online 10 March 2008

Keywords:
Additives
Electroplating conditions
Lead deposition
Lead dissolution

ABSTRACT

The structure of lead deposits (approximately 1 mm thick) formed in conditions likely to be met at the negative electrode during the charge/discharge cycling of a soluble lead-acid flow battery is examined. The quality of the lead deposit could be improved by appropriate additives and the preferred additive was shown to be the hexadecyltrimethylammonium cation, $C_{16}H_{33}(CH_3)_3N^+$, at a concentration of 5 mM. In the presence of this additive, thick layers with acceptable uniformity could be formed over a range of current densities (20–80 mA cm^{-2}) and solution compositions. While electrolyte compositions with lead(II) concentrations in the range 0.1–1.5 M and methanesulfonic acid concentrations in the range 0–2.4 M have been investigated, the best quality deposits are formed at lower concentrations of both species. Surprisingly, the acid concentration was more important than the lead(II) concentration; hence a possible initial electrolyte composition is 1.2 M Pb(II) + 5 mM $C_{16}H_{33}(CH_3)_3N^+$ without added acid.

1. Introduction

Earlier papers [1–4] have described preliminary studies of a soluble lead, flow battery where the electrode reactions are:

- negative electrode

$$Pb^{2+} + 2e^- \rightleftarrows Pb \quad (1)$$

- positive electrode

$$Pb^{2+} + 2H_2O \rightleftarrows PbO_2 + 4H^+ + 2e^- \quad (2)$$

and the overall reaction is

$$2Pb^{2+} + 2H_2O \underset{\text{discharge}}{\overset{\text{charge}}{\rightleftarrows}} Pb + PbO_2 + 4H^+ \quad (3)$$

The electrolyte is methanesulfonic acid in which Pb(II) is highly soluble (around 2.6 M). The key advantage of this battery, compared to other redox flow batteries, is that no membrane is required since there is a single electrolyte for the two electrode chemistries. The challenge becomes the need to control the form of both the lead and lead dioxide during a large number of charge/discharge cycles where thick layers are being deposited on both electrodes. For example, a 6-h charge at 50 mA cm^{-2} leads to deposits approximately 1 mm thick on each electrode (and the consumption of about 0.01 mol cm^{-2} of Pb(II) from solution).

This paper reports an investigation of the influence of electrolyte composition on the quality of the deposits. Clearly, it is advantageous that the discharged electrolyte contains a high concentration of Pb(II) and that, at the end of charge, this should be decreased to the lowest possible level in order to minimise the volume of electrolyte that needs be stored and circulated. Hence, the quality of the deposits over a range of Pb(II) concentrations was studied. It also has to be recognised that the lead and proton concentrations are not independent and the removal of 1 mole of Pb(II) during charge also leads to the formation of 2 mole of protons. For example, the complete charging of an initial electrolyte containing 2 M $Pb(CH_3SO_3)_2$ + 1 M CH_3SO_3H would result in a solution containing 5 M CH_3SO_3H. Hence the influence of acid concentration on the quality of the deposits also needs to be defined. The acid concentration, however, influences battery performance in other ways; when the acid concentration is high, the additional issues are electrolyte viscosity and the solubility of the Pb(II) [1]. In addition, towards the end of discharge, the acid concentration must remain sufficiently high to avoid the rate of lead dioxide reduction becoming a limiting factor. The acid concentration could also influence the rate of oxygen evolution:

$$2H_2O \rightarrow O_2 + 4H^+ + 4e^- \quad (4)$$

* Corresponding author. Tel.: +44 2380 593519.
E-mail address: dp1@soton.ac.uk (D. Pletcher).

0378-7753/$ – see front matter © 2008 Elsevier B.V. All rights reserved.
doi:10.1016/j.jpowsour.2008.02.024

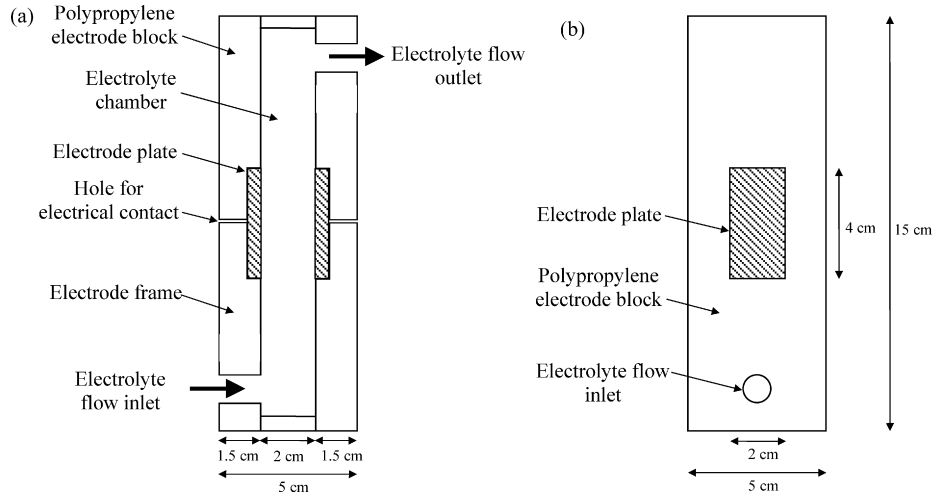

Fig. 1. A laboratory flow cell with 4 cm × 2 cm geometric area electrodes. (a) Cross-section of the cell, showing the essential components. The cell, which used flat silicone rubber gaskets, was sealed under compression by M6 steel tie bars (not shown). (b) Plan view of the electrode frame, showing the location of the 4 cm × 2 cm electrode plate.

as a competing reaction at the positive (lead dioxide) electrode during charge. The solutions with different Pb(II) and methanesulfonic acid concentrations studied in this work were selected to represent the electrolyte compositions likely to be met at different states of charge in a practical battery system with a high electrode area/electrolyte volume ratio.

Lead dendrites can occur under some conditions and the earlier paper reported the positive influence of ligninsulfonate as an additive [4]. There is also an extensive literature on additives for lead electroplating, electrowinning and electrorefining from acid electrolytes [5,6]. In the battery, however, it is essential that any additive for the negative electrode (a) is stable in high acid concen-

Table 1
Influence of additives on the form of the lead deposit and the current efficiency for the first charge/discharge cycle

Additive	Cell	Additive concentration	Deposit quality	% Coulombic efficiency
No additive	†		C	79
Hexadecyltrimethylammonium hydroxide	†	5 mM	A	93
Hexadecyltrimethylammonium tosylate	*	5 mM	A	
Hexadecyltrimethylammonium bromide	†	5 mM	D	31
Dimethyldodecylethylammonium hydroxide	†	5 mM	B	86
N,*N*-Dimethyldodecylamine *N*-oxide	*	5 mM	B	
Tetrabutylammonium hydroxide	†	5 mM	C	84
Dimethyldistearylammonium chloride	*	0.5 mM	D	
Benzylcetyldimethylammonium chloride	*	5 mM	B	
Hexadecyl trimethylammonium chloride	*	5 mM	D	
Benzethonium hydroxide	*	5 mM	A	
Benzyltrimethylammonium hydroxide	*	5 mM	C	
Sodium ligninsulfonate	†	1 g dm^{-3}	A	93
Sodium dodecylbenzenesulfonate	†	Satd.	C	86
Sodium dodecylsulfate	†	Satd.	C	87
1-Butyl-3-methylimidazolium 2-(2-methoxy-ethoxy)ethyl sulfate	†	5 mM	C	88
Sodium tosylate	†	5 mM	C	84
Polyvinylpyrrolidone	†	5 mM	D	89
Polyethylene glycol 20,000	†	1 g dm^{-3}	C	83
Polyethylene oxide 100,000	†	1 g dm^{-3}	C	85
Ethylenediamine	†	30 mM	C	84
Nonylphenyl polyethyleneglycol acetate	*	0.1 mM	D	
Glycolic acid ethoxylate 4-nonylphenyl ether	*	0.5 mM	A	
Brij™ 56	*	0.5 mM	B	
EMPIGEN™ BB detergent	*	5 mM	D	
Tyloxapol™	*	1 g dm^{-3}	A	
Triton™ X100	†	1 g dm^{-3}	A	93
Forafac™ 1098	†	2 g dm^{-3}	C	84
Zonyl™ FSO	†	2 g dm^{-3}	C	84
Zonyl™ FSK	†	2 g dm^{-3}	D	71
FC4430™	†	2 g dm^{-3}	D	74
Sodium metasilicate pentahydrate	†	5 mM	C	95
Co^{2+}	†	1 mM	C	88
Cd^{2+}	†	1 mM	C	88

The deposit qualities A–D are illustrated in Fig. 2. The cells and conditions used were: †, parallel plate flow cell (linear flow rate 4 cm s^{-1}) with a roughened carbon/polymer composite plate cathode. Current density: 20 mA cm^{-2} for 2 h. Electrode area: 8 cm^2. Electrolyte: 1.5 M $Pb(CH_3SO_3)_2$ + 0.9 M CH_3SO_3H (60 cm^3). Ambient temperature. *, parallel plate 'beaker' cell with magnetic stirrer bar (500 rpm) and expanded graphite plate cathode. Current density: 40 mA cm^{-2} for 2 h. Electrode area: 4 cm^2. Electrolyte 1.2 M $Pb(CH_3SO_3)_2$ + 0.2 M CH_3SO_3H (60 cm^3). Ambient temperature.

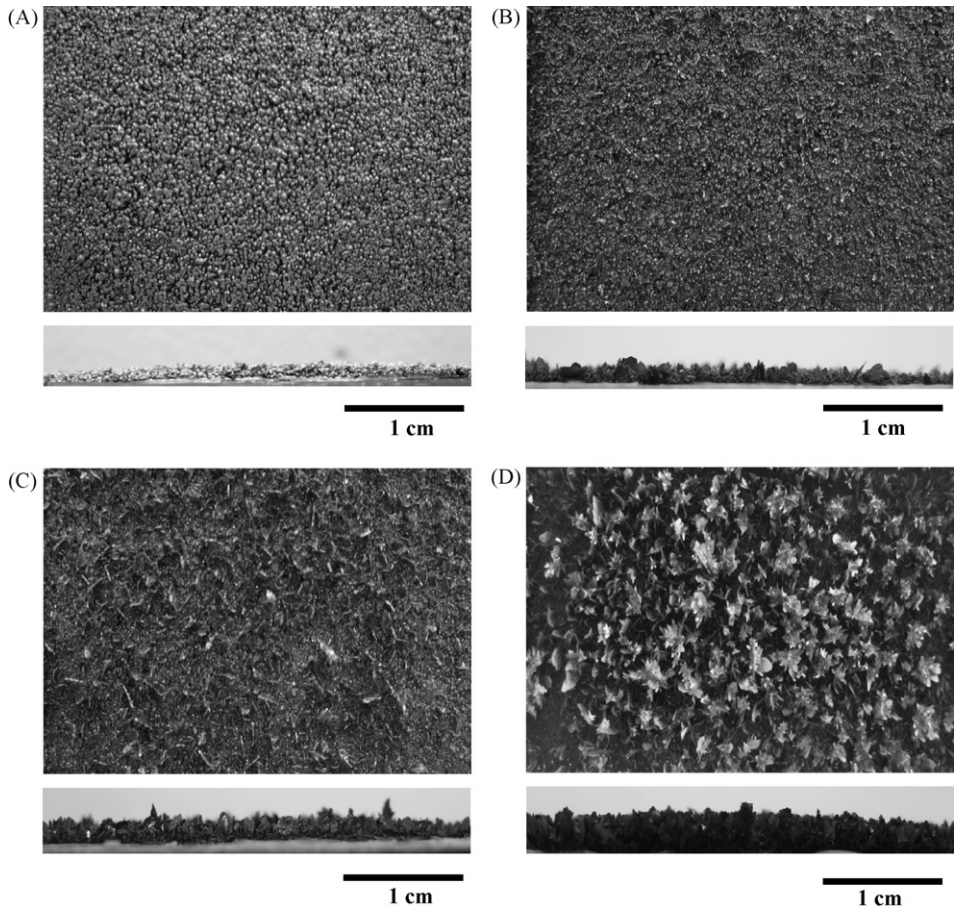

Fig. 2. Photographs of lead deposits to illustrate their quality. (A) Highest quality deposit, (B) some improvement compared to the absence of an additive, (C) no additive and (D) significantly worse than in the absence of additive. The electrodeposition conditions are set out in the legend to Table 1.

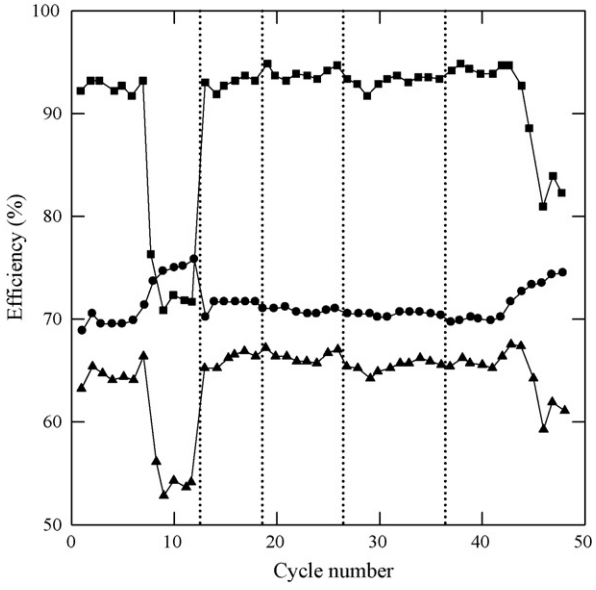

Fig. 3. Coulombic (■), voltage (●) and energy efficiency (▲) as a function of cycle number. The vertical dotted lines indicate that the electrolyte has been filtered. Cycle regime: charge at 20 mA cm^{-2} for 2 h and discharged at the same current density until the battery voltage dropped to 1.0 V. Small flow cell (electrode areas 8 cm^2) with scraped Ni foam negative electrode and roughened carbon/polymer composite positive electrode. Electrolyte flow rate: 4 cm s^{-1}. Electrolyte: 1.5 M $Pb(CH_3SO_3)_2$ + 0.9 M CH_3SO_3H + 5 mM $C_{16}H_{33}(CH_3)_3N^+$.

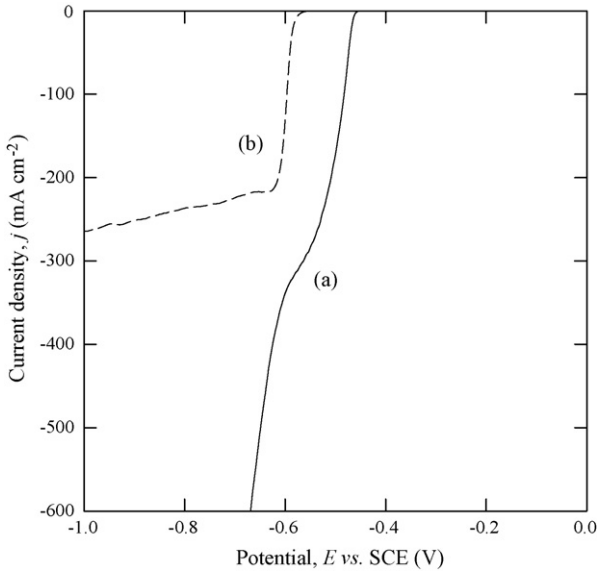

Fig. 4. Voltammograms recorded at a rotating vitreous carbon disc electrode in 0.5 M $Pb(CH_3SO_3)_2$ + 1.0 M CH_3SO_3H containing: (a) 0 mM and (b) 10 mM $C_{16}H_{33}(CH_3)_3N^+$. Rotation rate: 400 rpm. Potential scan rate: 20 mV s^{-1}.

trations, (b) does not oxidise at a lead dioxide anode and (c) does not adversely affect the quality of the lead dioxide deposit. Indeed, while ligninsulfonate inhibited the formation of dendrites, it also appeared to decompose during extended operation of the battery. This prompted an extensive study of electrolyte additives.

2. Experimental details

All solutions were prepared with water ($\ll 1\,\mu S\,cm^{-1}$) from a Whatman Analyst Purifier, methanesulfonic acid (Aldrich, 70 wt.%) and lead(II) oxide (Alfa Aesar, 99.9%). The lead methanesulfonate was formed by the reaction:

$$PbO + 2CH_3SO_3H \rightarrow Pb(CH_3SO_3)_2 + H_2O \quad (5)$$

using the calculated weight of lead oxide and volume of acid to obtain the desired electrolyte composition.

The Hull cell was a model TCACG 267 supplied by Kocour Inc. It had a lucite body with an electrolyte volume of 267 cm^3 and was fitted with carbon/composite electrodes having dimensions, 9 cm × 5 cm and 6 cm × 5 cm. A schematic of the flow cell is shown in Fig. 1. It has two electrodes, each having an area of 4 cm × 2 cm, and an interelectrode gap of 2.0 cm. The electrode materials were again carbon/polymer composites; in some experiments, the negative electrode had a fine nickel foam pressed into the carbon/polymer composite and then scraped to give a carbon surface with nickel protrusions [2]. The electrolyte volume circulated was 60 cm^3 and the mean linear flow velocity past the electrodes was 4 cm s^{-1}. The parallel plate 'beaker' cell was based on a square container 3.5 cm × 3.5 cm and 7.0 cm high and the electrolyte was stirred with a magnetic stirrer bar (500 rpm); the electrodes were expanded graphite plates with an area 1 cm × 4 cm. In all the experiments discussed in this paper, there is no significant change to the electrolyte composition during the timescale of the experiment due to the electrolyte volume/electrode area ratios employed. Hence, they should be regarded as a 'snapshot' in time during the charge or discharge of the battery.

Constant currents for experiments in the Hull and 'beaker' cells were obtained using a laboratory dc power supply from ISO-TECH model IPS2303. The flow cell experiments were controlled with an EG & G Potentiostat/Galvanostat model 263A and output data were recorded and analysed using EG & G Power Suite Software together with in-house software.

Scanning electron micrographs were obtained using two instruments. Samples from the Hull cell were analysed using a JEOL SEM model JSM-5910 using an accelerating voltage of 15 kV. The other samples were analysed using a Phillips Environmental SEM model XL30 again using an accelerating voltage of 15 kV. The samples were mounted at 90° to the beam.

3. Results and discussion

3.1. Additives for lead deposition

The ability to deposit lead as a uniform layer during extended deposition times and over a range of current densities was considered essential to successful long term battery operation. In particular, dendrite formation and growth across the interelectrode gap must be avoided. Hence, a large number of additives were examined to define their influence on the quality of the deposit.

The initial series of experiments was carried out in two different cells and employing two slightly different electrolytes but check experiments indicated that, in general, the conclusions were the same under both conditions. Table 1 reports the compounds studied together with their effect on the deposit quality and, in some cases, the current efficiency during a first charge/discharge cycle. The photographs of the deposits in Fig. 2(A)–(D) are intended to illustrate the quality of the lead deposits obtained. In the absence of an additive, see Fig. 2(C), the deposit is composed of intergrowing lead crystallites; the layer is not completely uniform and some protrusions towards the positive electrode are clearly visible. Many of the compounds studied had little or no influence on the deposit quality. A few of the possible additives had the effect of making the deposit quality worse and certainly unacceptable in a secondary battery; this is illustrated in Fig. 2(D) where structured growths and/or dentrites are clearly visible and the cross-sectional view shows that the deposit is thicker and much less compact. Another group of the compounds improved the deposit quality and typical deposits are shown in Figs. 2(A) and (B). These included long chain tetraalkylammonium cations, Triton™ X 100, Brij™56, Tyloxapol™ and sodium ligninsulfonate. In the case of the best deposits, Fig. 2(A), the crystallite size is smaller and more uniform and the deposit appears uniform and free of protrusions over the entire surface. The cross-sectional image shows that the deposit is thin and compact. Interestingly, the current efficiency is acceptable for the first charge/discharge cycle of the small battery with electrolytes containing almost all the additives; not surprisingly, the exception is the solution where bromine can be formed via oxidation of bromide ions during charge.

Several of the additives were selected for more extensive charge/discharge cycling in the small flow cell (electrode area 8 cm^2, electrolyte volume 60 cm^3). The electrolyte was 1.5 M $Pb(CH_3SO_3)_2$ + 0.9 M CH_3SO_3H and, in each cycle, the battery was charged at 20 mA cm^{-2} for 2 h then discharged at the same current density until the battery voltage dropped to 1.0 V. In the absence of an additive, the battery can be cycled but the efficiency drops with cycle number and a black powdery deposit (shown by X-ray diffraction to be largely lead dioxide) accumulates in the electrolyte over the first 10 cycles; eventually shorting of the electrodes occurs. Several of the promising additives, e.g. Triton™ X 100 and sodium ligninsulfonate, however, contain functional groups that potentially could be oxidised at the lead dioxide electrode. Indeed, when batteries with electrolytes containing such additives were cycled, the electrolyte was observed to change colour and their effectiveness in controlling the deposit quality decreased with cycling. The long chain tetraalkylammonium cations appeared to be the preferred

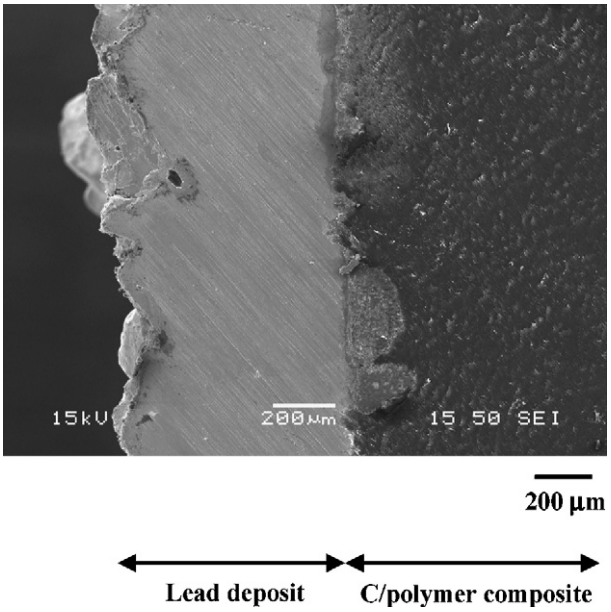

Fig. 5. SEM of a cross-section of a lead deposit on a scraped, carbon/high density polyethylene composite cathode. Current density: 150 mA cm^{-2} for 2 h. Electrolyte: 0.5 M $Pb(CH_3SO_3)_2$ + 0.3 M CH_3SO_3H + 5 mM $C_{16}H_{33}(CH_3)_3N^+$. Cell: parallel plate 'beaker' cell with magnetic stirrer bar (500 rpm). Ambient temperature.

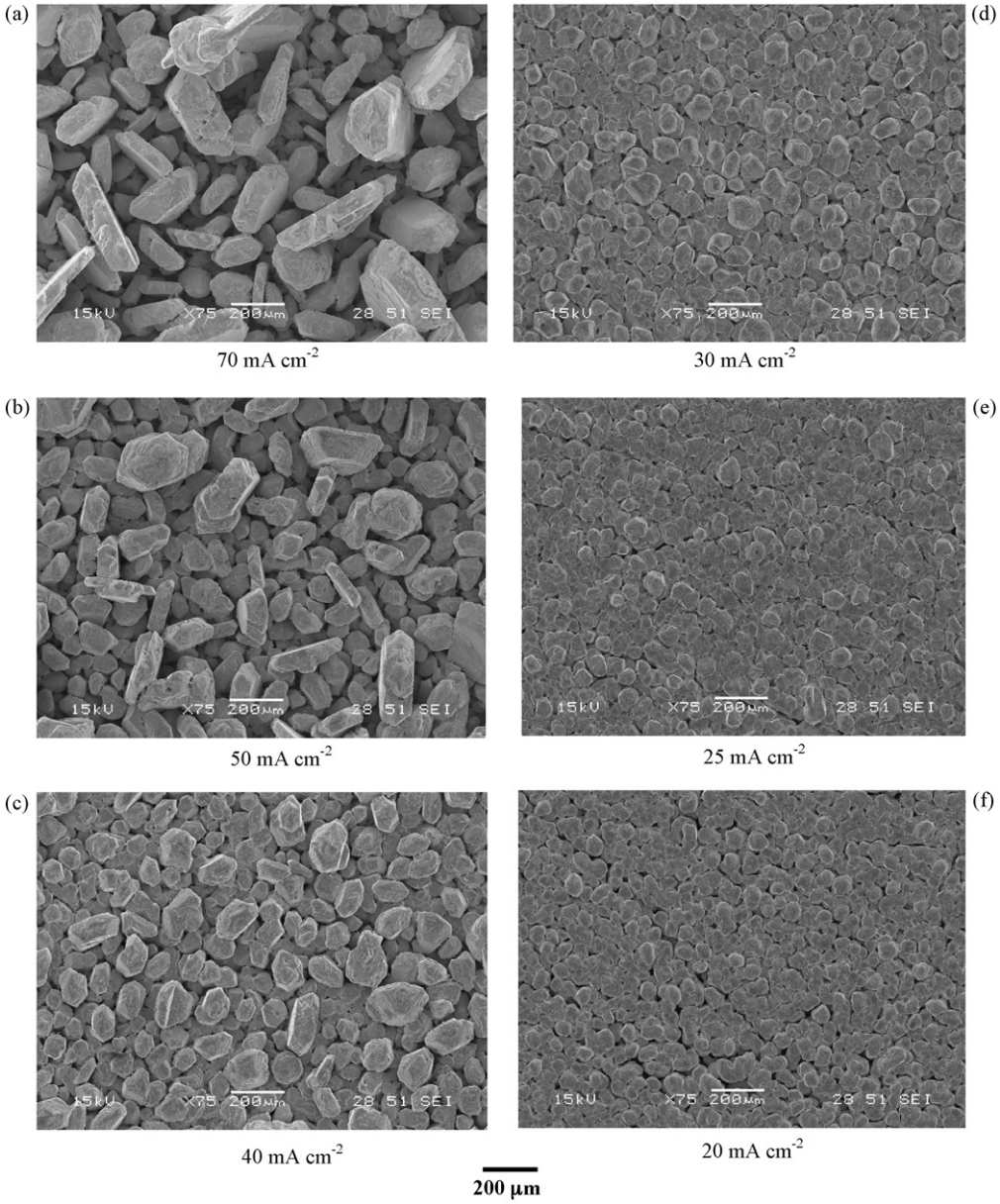

Fig. 6. SEM pictures of lead deposits as a function of current density. Hull cell with a scraped, carbon/high density polyethylene composite cathode. Deposition time: 2 h. Electrolyte: 0.5 M $Pb(CH_3SO_3)_2$ + 1.0 M CH_3SO_3. Ambient temperature.

additive and later experiments mainly used the hexadecyltrimethylammonium cation as the additive.

Fig. 3 reports the performance of the small flow battery with electrolyte containing 5 mM hexadecyltrimethylammonium methanesulfonate. The battery maintained its performance until the experiment was terminated after 48 cycles (2 h charge followed by discharge to a cut-off battery voltage of 1 V) in order to release the equipment for other experiments. With this electrolyte, a very small amount of the black powder was evident in the electrolyte; it was essential to periodically filter the electrolyte in order to maintain the negative electrode deposit quality and battery deposit; a small amount of solids in the electrolyte led to a rapid decline in battery performance. Filtering of the electrolyte is indicated in the figure by the dotted lines. Fig. 3 reports the overall energy efficiency as well as the coulombic and voltage efficiencies. The coulombic efficiency is generally above 90% but drops suddenly if the black powdery lead dioxide is not removed by filtration while the voltage efficiency remains close to 70%. In all experiments, it was found that a small amount of the lead dioxide free in the solution had an adverse effect on the quality of the lead deposited on the negative electrode. The energy efficiency follows the variation of coulombic efficiency but could be maintained at around 65% if the electrolyte was filtered. There was no loss in performance when the experiment was terminated. Of course, this battery performance demonstrates that the positive electrode is also performing well and that the lead dioxide formed efficiently and almost all adhered well to the electrode. Further results on the positive electrode will be reported elsewhere [7]. It should also be noted the good quality lead deposits could be obtained with a number of current collector materials including nickel, nickel foam materials, carbon materials and carbon/polymer composites.

The influence of the hexadecyltrimethylammonium cation on the form of the deposit can also be seen from voltammetry. Fig. 4 shows voltammograms recorded at a rotating vitreous carbon disc electrode in a solution containing 0.5 M $Pb(CH_3SO_3)_2$ + 1.0 M CH_3SO_3H with and without additive. In the

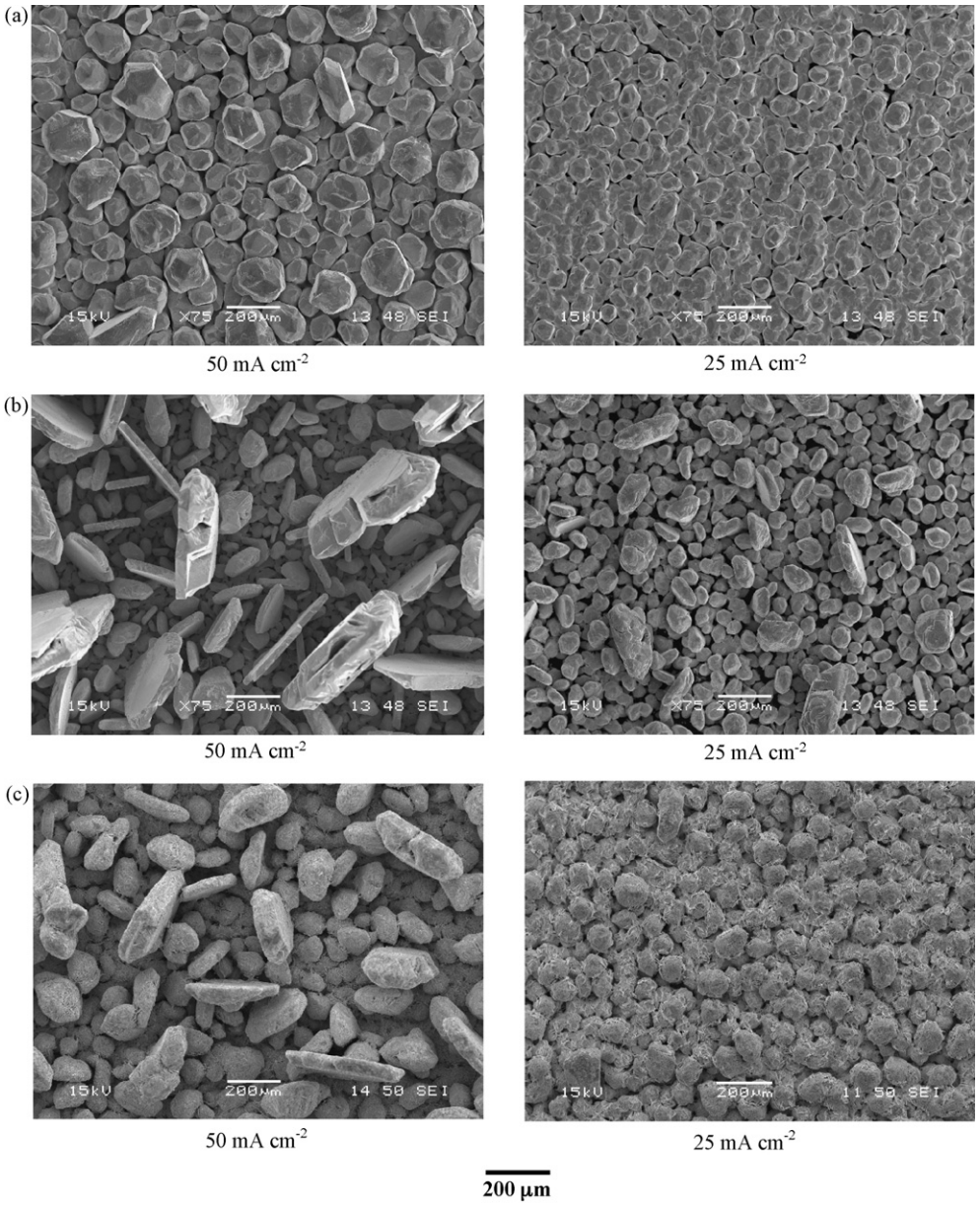

Fig. 7. SEM pictures of lead deposits at two current densities from (a) 0.5 M $Pb(CH_3SO_3)_2$ + 1.0 M CH_3SO_3H + 5 mM $C_{16}H_{33}(CH_3)_3N^+$, (b) 1.5 M $Pb(CH_3SO_3)_2$ + 1.0 M CH_3SO_3H + 5 mM $C_{16}H_{33}(CH_3)_3N^+$ and (c) 1.5 M $Pb(CH_3SO_3)_2$ + 1.0 M CH_3SO_3H + 20 mM $C_{16}H_{33}(CH_3)_3N^+$. Hull cell with a scraped, carbon/high density polyethylene composite cathode. Deposition time: 2 h. Ambient temperature.

presence of 10 mM $C_{16}H_{33}(CH_3)_3N^+$, a well formed reduction wave is seen at $E_{1/2}$ = −0.61 V *vs.* SCE and the limiting current density has the value expected for a mass transport controlled reduction of the lead(II). In the absence of the additive, the plateau to a wave is only seen as a point of inflection and there is a further, immediate rapid rise in current density. This is due to a rapid increase in the area of the lead deposit including the formation of dendrites around the edge of the disc. It can also be seen that the $C_{16}H_{33}(CH_3)_3N^+$ inhibits the lead deposition; the presence of the additive shifts the commencement of lead deposition negative by approximately 110 mV. This implies that the hexadecyltrimethylammonium cation adsorbs on the electrode surface.

It was also noted that the hexadecyltrimethylammonium cation had little effect on the open circuit voltage of the soluble lead-acid battery. For example, in a battery with an electrolyte containing 0.5 M $Pb(CH_3SO_3)_2$ + 1.0 M CH_3SO_3H, the open circuit voltage was 1.673 V and the value dropped to 1.669 V and 1.666 V in the presence of 5 mM and 30 mM $C_{16}H_{33}(CH_3)_3N^+$, respectively.

A thick lead deposit was grown onto a scraped carbon/high density polyethylene composite cathode using a current density of 150 mA cm^{-2} for 2 h and an electrolyte consisting of 0.5 M $Pb(CH_3SO_3)_2$ + 0.3 M CH_3SO_3H + 5 mM $C_{16}H_{33}(CH_3)_3N^+$. Fig. 5 shows a cross-section image of the lead layer obtained by SEM. Because lead is a soft metal, the cross-section could not be polished after cutting and hence some structure may be lost. Even so, it is clear that even at this high current density, the lead layer is compact and strongly adherent to the scratched carbon/polymer composite substrate. Indeed, this appears to be a very satisfactory deposit for battery operation.

3.2. The influence of lead(II) and methanesulfonic acid concentrations

In order to define the influence of current density as well as electrolyte composition on the morphology of the lead deposit, a number of experiments were carried in a Hull cell with a scraped

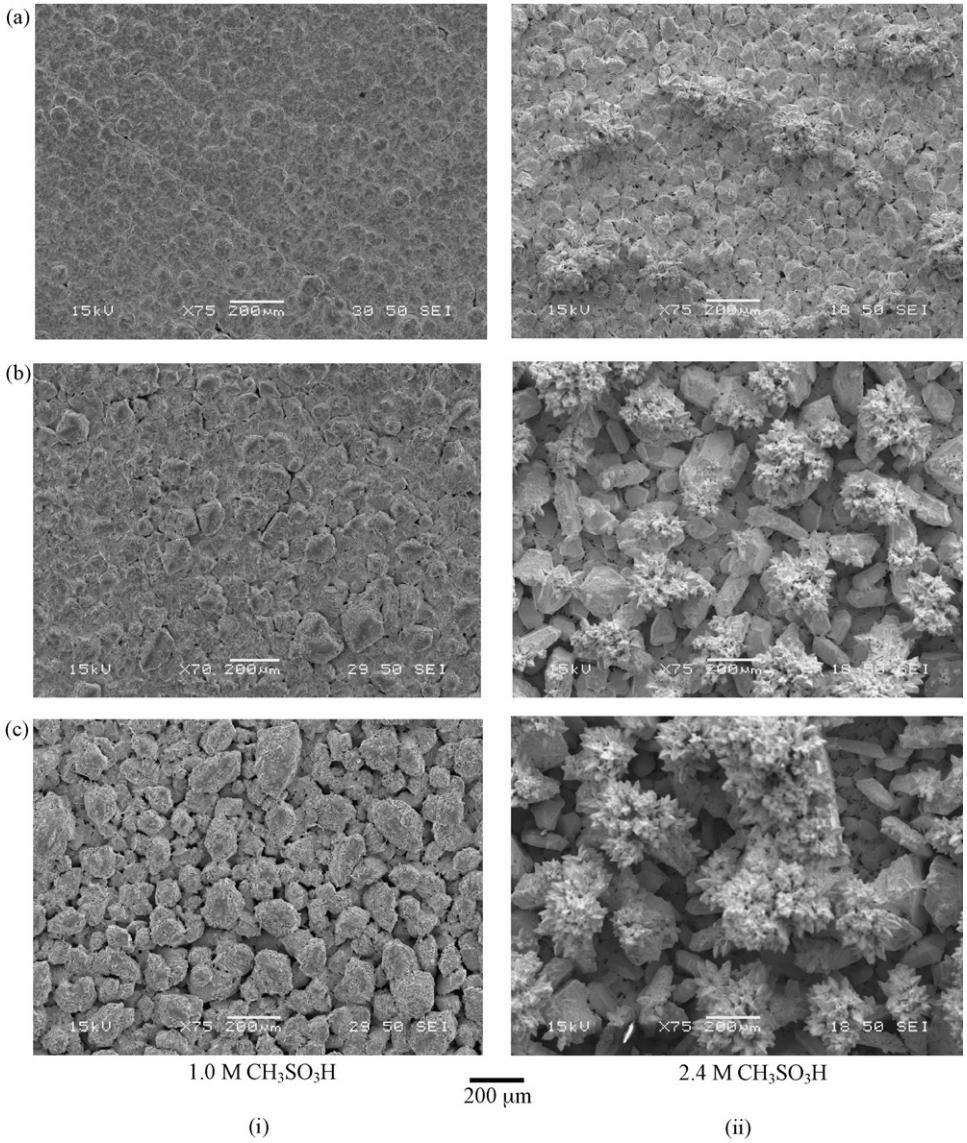

Fig. 8. Comparison of deposits from deposition of lead from electrolytes containing (i) 1.0 M CH_3SO_3H and (ii) 2.4 M CH_3SO_3H. Both also contained 0.3 M $Pb(CH_3SO_3)_2$ + 5 mM $C_{16}H_{33}(CH_3)_3N^+$. (a) 25 mA cm^{-2}, (b) 50 mA cm^{-2} and (c) 70 mA cm^{-2}. Hull cell with a scraped, carbon/high density polyethylene composite cathode. Deposition time: 2 h. Ambient temperature.

carbon/high density polyethylene composite cathode. In fact, the cell gave a current density range of approximately 10–80 mA cm^{-2} across the cathode with the electrolytes used. The deposition time was 2 h and, of course, the deposit thickness across the cathode is proportional to the local current density.

In the first experiment, the electrolyte was 0.5 M $Pb(CH_3SO_3)_2$ + 1.0 M CH_3SO_3H, without additive. Over the whole cathode surface, the lead deposit adhered well and appeared, by eye, to be very satisfactory. At all current densities, deposit was compact and has a silvery colour. Fig. 6 shows a set of SEM pictures taken at various points across the Hull cell cathode. At this magnification, it is apparent that over the lower current density range 20–30 mA cm^{-2}, the deposits were similar and consisted of closely packed, overlapping small centres with an approximately hemispherical shape. Only a few void areas were visible. With increasing current density, the deposit became rougher and by 30 mA cm^{-2} there is evidence that there is nucleation and growth of secondary layers. At higher current density, at least the top layer, consisted of angular lead crystals with dimensions which increase with current density (hence also amount of lead deposited) and could reach hundreds of microns. By 70 mA cm^{-2}, the surface was dominated by randomly orientated, large crystals of variable dimensions.

Fig. 7 reports the influence of increasing the lead(II) concentration from 0.5 M to 1.5 M and also the effect of the additive, $C_{16}H_{33}(CH_3)_3N^+$, while maintaining the same initial acid concentration; two current densities are shown to illustrate the trends. Comparison of the SEM images of the deposits, Fig. 7(a) with Fig. 6(b) and (e), shows the influence of 5 mM $C_{16}H_{33}(CH_3)_3N^+$ with 0.5 M lead(II). With a deposition current density of 25 mA cm^{-2}, the deposits were similar, with and without additive. On the other hand, at 50 mA cm^{-2} the additive produced a significant improvement, the crystals being more uniform in size and less angular. The improvement becomes more marked at even higher current densities. The additive can be seen to control the size of the lead crystals and also the rate of nucleation of further crystallites, thereby limiting secondary growth and giving a substantially more uniform deposit. The improvement in deposit quality on addition of the $C_{16}H_{33}(CH_3)_3N^+$ could also be seen by eye as it significantly increases the reflectivity of the deposit.

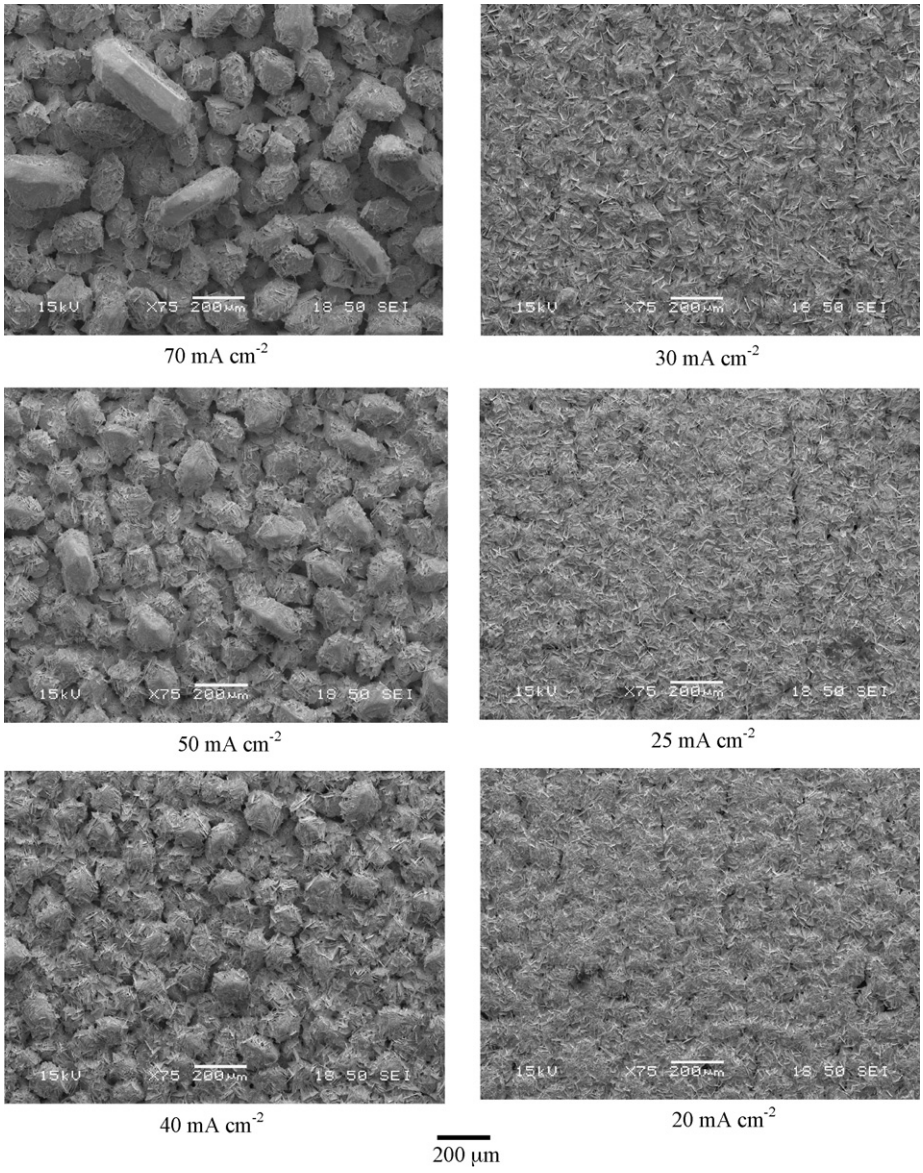

Fig. 9. SEM pictures of lead deposits as a function of current density. Hull cell with a scraped, carbon/high density polyethylene composite cathode. Deposition time: 2 h. Electrolyte: 1.5 M $Pb(CH_3SO_3)_2$ + 5 mM $C_{16}H_{33}(CH_3)_3N^+$ (no acid added). Ambient temperature.

At the higher lead(II) concentration, the deposits appeared, by eye, to be less shiny and became matte at the higher current densities. Fig. 7(a) and (b) presents SEM images of the deposits from the two lead(II) solutions, 0.5 M and 1.5 M Pb(II), with the same additive concentration (5 mM). At a 1.5 M lead(II) concentration, Fig. 7(b), the deposit formed angular lead crystals at lower current density and the crystals grew larger; there was a clear trend for the deposit to be more disordered at the higher concentration of lead(II). Even so, and as reported above in the discussion of Fig. 3, these deposits were not necessarily unsatisfactory in the battery; with 1.5 M lead(II) the battery could be cycled 50 times without loss in performance. Fig. 7(c) shows the effect of increasing the concentration of $C_{16}H_{33}(CH_3)_3N^+$ from 5 mM to 20 mM in the solution containing 1.5 M lead(II). The deposit quality was significantly improved with the higher additive concentration although it remained not as good as with 0.5 M lead(II) containing 5 mM $C_{16}H_{33}(CH_3)_3N^+$. At low current density and 1.5 M lead(II), there appeared to be secondary growth on the compact, hemispherical structure while at higher current density the lead crystals were larger and more disordered. With all electrolyte compositions and at the higher current densities, the trend to surfaces with large lead crystals and a distribution of lead crystallite sizes and orientations became more evident. It was also found that the deposits become less uniform with deposition time. Hence, deposition charge and therefore thickness of the deposit was an important factor in determining deposit quality.

The influence of acid concentration was then investigated in the Hull cell. Fig. 8 shows the surfaces produced with a relatively low lead(II) concentration (0.3 M) but two different methanesulfonic acid concentrations (+5 mM $C_{16}H_{33}(CH_3)_3N^+$). With the electrolyte containing 1 M acid, good quality lead deposits were obtained at all current densities. Indeed, at low current densities, the deposits were very uniform with no voids. In the electrolyte containing 2.4 M acid, the deposits were substantially poorer in quality. With a deposition current density of 70 mA cm^{-2}, a lot of secondary growth was observed on relatively large lead crystals. This was also evident at 50 mA cm^{-2} and even at 25 mA cm^{-2}, the deposit was non-uniform and clearly composed of angular lead crystals. The decay in deposit quality with increasing acid concentration was particularly evident above a critical level of about 2 M.

The trend to higher quality deposits with low acid concentrations was confirmed by a Hull cell experiment with an electrolyte initially containing 1.5 M $Pb(CH_3SO_3)_2$ + 5 mM $C_{16}H_{33}(CH_3)_3N^+$ but zero acid. Fig. 9 reports SEM images of the deposits. A rather uniform and dense deposit was formed at all the current densities. At low current densities, the deposits appeared to be made up of closely spaced, overlapping hemispherical centres while angular lead crystals predominated at the higher current densities. At all current densities investigated, there was evidence of fine secondary growths over the surface but there was no indication that these led to dendrites.

4. Conclusions

In this paper we have focused on studies of the lead deposit at the negative electrode at electrolyte compositions likely to be met in a soluble lead(II) flow battery. It was confirmed that electrolytes based on lead(II) in methanesulfonic acid allowed the electrodeposition of thick layers of lead over a range of current densities. The quality of the deposits was significantly improved by the presence in the electrolyte of certain additives and the preferred additive was the hexadecyltrimethylammonium cation, $C_{16}H_{33}(CH_3)_3N^+$, at a concentration of approximately 5 mM; this additive improved the uniformity and smoothness of the lead deposit without adversely affecting the positive electrode [7]. In electrolytes containing the additive, the lead deposits appeared suitable for battery operation over a very wide range of lead(II) and methanesulfonic acid concentrations. The trend was, however, for the brightest and smoothest deposits to be formed when the lead(II) and methanesulfonic acid are present only in modest concentration. As the lead(II) and methanesulfonic acid concentrations were increased the deposits became less uniform and ordered and this trend was most prevalent at the higher current densities. Moreover, the influence of the acid concentration was stronger than that of the lead(II) ion and we would be cautious about allowing the acid concentration to increase above 2 M during battery charging. Bearing in mind the other requirements of a flow battery electrolyte, a possible electrolyte for newly installed batteries would be 1.2 M Pb(II) + 5 mM $C_{16}H_{33}(CH_3)_3N^+$ without added acid; it might then be cycled between 0.2 M Pb(II) + 2 M CH_3SO_3H at top of charge to and 1.15 M Pb(II) + 0.1 M CH_3SO_3H at bottom of charge. Also the current density for lead deposition could be up to 100 mA cm^{-2}. These conclusions will be examined in larger cells with electrode area to electrolyte volume ratios that allow large swings in electrolyte compositions; such cells are presently under construction.

Throughout this study, successful operation required careful measures to avoid 'edge effects'. For example, where non-uniform deposits were found during the studies of additives, the worst deposits, and often dendrites, were clearly observed at the very edges of the electrodes. Similarly, when failure occurred during flow battery cycling, extended growth and/or dendrites at the electrode edge were often the cause. In consequence, we believe that the avoidance of edge effects is essential to successful battery scale-up. Part of the overall programme is the application of modelling and experimental studies to ensure uniform mass transport and current distribution over all the electrode in the larger cells which are under design and construction.

Acknowledgements

This work has been funded in part by the DTI Technology Programme Contract TP/4/EET/6/I/2296 entitled '*Redox Flow Cells for Intelligent Grid Management*'. The authors would like to thank the project partners, especially John Collins and Duncan Stratton-Campbell of C-Tech Innovation Ltd, for helpful comments.

References

[1] A. Hazza, D. Pletcher, R. Wills, Phys. Chem. Chem. Phys. 6 (2004) 1773.
[2] D. Pletcher, R. Wills, Phys. Chem. Chem. Phys. 6 (2004) 1779.
[3] D. Pletcher, R. Wills, J. Power Sources 149 (2005) 96.
[4] A. Hazza, D. Pletcher, R. Wills, J. Power Sources 149 (2005) 103.
[5] A.T. Kuhn (Ed.), The Electrochemistry of Lead, Academic Press, New York, 1979.
[6] M. Schlesinger, M. Paunovic (Eds.), Modern Electroplating, The Electrochemical Society, Pennington, 2000.
[7] D. Pletcher, H. Zhou, G. Kear, C.T.J. Low, F.C. Walsh, R.G.A. Wills, J. Power Sources, doi:10.1016/j.jpowsour.2008.02.025.